Applied Catalysis A: General 464–465 (2013) 101–108

Contents lists available at SciVerse ScienceDirect

Applied Catalysis A: General

journal homepage: www.elsevier.com/locate/apcata

Promoting effect of ZrO_2 carrier on activity and thermal stability of CeO_2-based oxides catalysts for toluene combustion

Han-Feng Lu*, Ying Zhou, Wen-Feng Han, Hai-feng Huang, Yin-Fei Chen*

College of Chemical Engineering and Material Science, Institute of Catalytic Reaction Engineering, Zhejiang University of Technology, Hangzhou 310014, China

ARTICLE INFO

Article history:
Received 27 January 2013
Received in revised form 19 April 2013
Accepted 25 May 2013
Available online xxx

Keywords:
CeO_2-based oxides
Carrier effect
Thermal stability
Catalytic combustion
Toluene

ABSTRACT

ZrO_2 was used as a support for the preparation of Cu–Mn–Ce mixed oxides catalysts (CMC) by impregnation method and calcination at different temperatures. A model reaction, toluene combustion was conducted to evaluate the performance of CMC/ZrO_2 catalysts. High thermal stability and activity was obtained on these catalysts. The effects of CMC loading and calcination temperature on the structure and redox properties of catalysts were also investigated by XRD, H_2-TPR, TEM and XPS. Results show that calcination leads to the interaction of ZrO_2 and CMC via the formation of a new phase of $Zr_{0.88}Ce_{0.12}O_2$ in the interface, which is more likely to be formed in the catalysts with low CMC loading levels. $Zr_{0.88}Ce_{0.12}O_2$ seems to function as the actual carrier of active phase of CMC, which cannot only stabilize the surface active structure of CMC but also enhance the mobility of active oxygen and improve the catalytic performance of total oxidation as well.

1. Introduction

Cerium dioxide (CeO_2) doped with specific transition metal ions (such as Cu, Mn and Co) with the formation of ceria-based solid solution structure or mixed oxides is a very promising catalytic material, and they are widely used for the abatement of various air pollutants including volatile organic compounds (VOCs) [1–6], NO_x [7,8] and soot [9–11]. However, these mixed oxides catalysts often show relatively low thermal stability following calcination at temperatures above 600 °C [12,13], which has become a main impediment in the application of the catalysts in the areas of environmental protection.

The thermal sintering mechanism of metal oxides is more complicated than that of precious metal catalysts. At high temperatures, metal oxides undergo various structural/chemical changes, such as rearrangement of solid-phase structural, decrease in lattice defects, atomic migration and alteration in metal ionic valences. These changes are usually followed by the decreases in surface area and catalytic activity of metal oxides [14,15]. Especially for CeO_2-based oxides catalysts, their active structures depend on lattice defects and ion vacancies, which are formed by the doping of transition mental ions. These defects and vacancies provide major transfer channels for surface oxygen (O_2^-, O^-), lattice oxygen (O^{2-}) and are responsible for the high catalytic activity at low temperatures [6,16]. On the other hand, these defects and vacancies also can function as channels for diffusion sintering, i.e., in these channels, metal ions facilely migrate and change in valence, resulting in a decrease in surface areas and activities [12,17]. For this reason, usually, it is difficult for CeO_2-based oxide catalysts to achieve high catalytic activity and high thermal stability at the same time.

Effective control of the atomic migration and the growth of size of nanocrystals at high temperatures is a major challenge for the design of CeO_2-based oxides catalysts. The incorporation of structural additives (Al, Zr, La and Y) into CeO_2 lattice was found to be a simple and feasible way to isolate the nonparties and delay sintering at high temperatures [12,15,18–20]. Ce–Zr–O solid solution with high thermal stability is widely used in the three way catalysts for the treatment of automotive exhaust [21–23]. Unfortunately, excessive amounts of additives usually tend to damage the original active structure of CeO_2-based mixed oxides and consequently reduce the activity of catalysts.

In order to maintain the original active structure and activity, the CeO_2-based oxides catalysts also is supported on some metal oxides (Al_2O_3, SiO_2 and SBA-15 etc.) with high surface area, which can stabilize the active phase through surface dispersion and prevention of atom migration at high temperatures [17,24–28]. For example, Wu et al. [17] reported that the introduction of Al_2O_3 into MnO_x–CeO_2 catalyst markedly increased the textural stability with a relatively high dispersion of MnO_x and CeO_2. Reddy et al. [28] found that CeO_2 solid solutions deposited over SiO_2 surface

* Corresponding authors at: Zhejiang University of Technology, 18 Chaowang Road, Hangzhou 310014, PR China. Tel.: +86 571 88320767; fax: +86 571 88320767.
E-mail addresses: luhf@zjut.edu.cn, lu.hanfeng@gmail.com (H.-F. Lu), yfchen@zjut.edu.cn (Y.-F. Chen).

0926-860X/$ – see front matter © 2013 Elsevier B.V. All rights reserved.
http://dx.doi.org/10.1016/j.apcata.2013.05.036

exhibited high thermal stability and revealed a substantial enhancement in the oxygen vacancy concentration. However, to the best of our knowledge, there are few reports on the use of ZrO_2 as support for CeO_2-based oxides. It necessitates the study about the strong interaction of CeO_2-based oxides with ZrO_2 as they have similar ionic radius, which leads to the expectation of high thermal stability and activity of catalysts.

In the present work, a novel type of mixed ceria-based oxides catalyst (consisting of Cu, Mn and Ce, abbreviated as CMC) with ZrO_2 as support were prepared by impregnation method and tested in catalytic combustion of toluene. This study focuses on two major issues: (i) The activity and thermal stability of the catalysts with different CMC loadings; (ii) The support effect of ZrO_2 on the structure features, redox properties and active oxygen species.

2. Experimental

2.1. Catalyst preparation

Hydrous zirconia was prepared by dropwise adding a solution of $ZrOCl_2$ (0.15 M) into a rigorously stirred ammonium solution (5.0 vol%) at room temperature. The pH value during precipitation was carefully controlled at 10. The precipitate formed as described above was collected by filtering and washing with deionized water until there was no detectable Cl^-. Then it was dried at 110 °C and calcined at 500 °C, leading to the ZrO_2 support with BET surface area of 65 m^2/g. Samples of CMC/ZrO_2 were prepared by loading the support with appropriate amounts of CuO, MnO and CeO_2 by impregnation method with Cu, Mn and Ce nitrates as precursors (molar ratio of Cu/Mn/Ce is 1/2/4), and the concentrations of these precursors were adjusted to yield catalysts with nominal loadings of Cu–Mn–Ce 2.5, 5, 10, 20 and 40 wt% (the loading amount was calculated by the weight of CuO, MnO and CeO_2). The catalysts were dried at 110 °C and calcined at temperatures of 500, 650, 800, 900 and 1000 °C for 3 h in flowing air respectively. As a comparison, samples of CMC/TiO_2 with 5% and 20% CMC loading were also prepared following the same method.

2.2. Characterization

2.2.1. BET specific surface area

Specific surface area of catalyst was measured by the BET method from the nitrogen adsorption isotherms. The experiments were carried out on a micromeritics ASAP 2020 instrument at 77 K. Prior to the experiments, samples were degassed at 427 K for 3 h.

2.2.2. X-ray diffraction (XRD)

XRD data of the samples were collected on a SCINTAG XTRA X-ray diffractometer equipped with Ni filtered Cu Kα (λ = 1.542 Å, 40 kV) radiation. The measurements were conducted in the 2θ range of 10–60° with a step size of 0.033°.

2.2.3. Temperature programmed reduction (TPR)

TPR experiments were performed on a Fine-Tech Autochem 3010E instrument. A desired amount of the samples (200 mg) was placed in a quartz reactor, pretreated in a flow of Ar gas at 250 °C for 2 h, and cooled to 70 °C. A gas mixture of H_2 (5%)-Ar (95%) was then passed (30 ml/min) through the reactor. The temperature was increased from 70 °C to 750 °C at a heating rate of 10 °C/min. A TCD detector was employed at the outlet of the reactor to measure the volume of hydrogen consumed during reduction.

2.2.4. X-ray photoelectron spectroscopy (XPS)

A spectrometer from Kratos AXIS Ultra DLD photoelectron spectroscopy with a monochromatized microfocused Al X-ray source was employed. Charging of samples was corrected by setting the binding energy of adventitious carbon (C 1s) at 284.6 eV. Prior to the measurements, the powder sample, pressed into self-supporting disks, was loaded into a sub-chamber and then evacuated for at 25 °C 4 h.

2.3. Catalytic activity measurement

Catalytic combustion of toluene was conducted on a fixed-bed quartz tube reactor (i.d. 10 mm) at atmospheric pressure. 500 mg catalyst was packed at the isothermal zone of the reactor. The feed (0.5 vol% toluene in air) was introduced to the catalyst at a flow rate of 200 mL/min (gas hourly space velocity (GHSV) = 24,000 mL h^{-1} (gcat.)$^{-1}$). The reactor effluent was analyzed on line at desired temperatures by HP 6890 gas chromatography equipped with an FID detector.

3. Results and discussion

3.1. Catalytic activity test

The results of catalytic activities in toluene combustion over CMC/ZrO_2 with different CMC loadings are shown in Fig. 1. No organic products of partial oxidation were observed during the catalytic combustion of toluene. The activity of catalyst calcined at temperature of 500 °C increases with CMC loading. When the loading of CMC is higher than 5%, the catalysts exhibit satisfactory catalytic performance, with T_{90} (the temperature needed for 90% toluene conversion) below 240 °C. The most active catalysts are 20% and 40% CMC/ZrO_2 catalysts which exhibit much lower "light-off" temperatures and their T_{90} are only 205 °C and 200 °C, respectively. It is competitive to those of conventional precious metal catalysts such as supported Pd and Pt reported by Luo et al. [29] and Saqer et al. [30] whose T_{90} are about 200 °C, and the perovskites [31,32] whose operating temperature is in the range of 260–300 °C at a similar space velocity. However, with the increase in calcination temperature, the catalysts with higher loadings of CMC show more rapid deactivation. T_{90} of 20% and 40% CMC/ZrO_2 catalysts dramatically increase to above 350 °C following calcinations at 900 °C, respectively. Among all the catalysts studied, 5% CMC/ZrO_2 shows the best balance between of thermal stability and activity. Its T_{90} (270 °C) keeps almost unchanged after calcination in the range of 650–900 °C. In addition, compared with the calcination at 500 °C, the rate of toluene combustion is further accelerated for 5% CMC/ZrO_2 catalyst calcined at higher temperatures. However, deactivation is also detected when 5% CMC/ZrO_2 catalyst was calcined at temperatures up to 1000 °C. We suggest that there is an optimal loading of CMC over ZrO_2. According to the results, it could be the key point to achieve high activity and thermal stability at the same time. This insight is also helpful for the preparation of suitable CeO_2-based mixed oxides catalyst under different reaction conditions.

The surface area of metal oxides catalyst was considered as a very important factor determining its activity [33,34]. The specific surface areas of 40% CMC/ZrO_2 rapidly decreases from 47.2 m^2/g to 0.46 m^2/g with increase of calcination temperature from 500 °C to 900 °C, indicating the growth of nanocrystal of the catalyst. However, for 5% CMC/ZrO_2, although its surface area decreases from 52.3 to 11.5 m^2/g (see Table 1), the activity maintains almost the same even with calcinations at temperatures from 650 to 900 °C. This suggests that more active sites are formed to compensate the decrease in surface area during high temperature calcinations.

Fig. 1 seems to imply that ZrO_2 stabilizes the active phase of CMC via surface dispersion and prevents them from migrating at high temperatures. To confirm the dispersion effect of support, an anatase TiO_2 which was considered as a good carrier for mixed

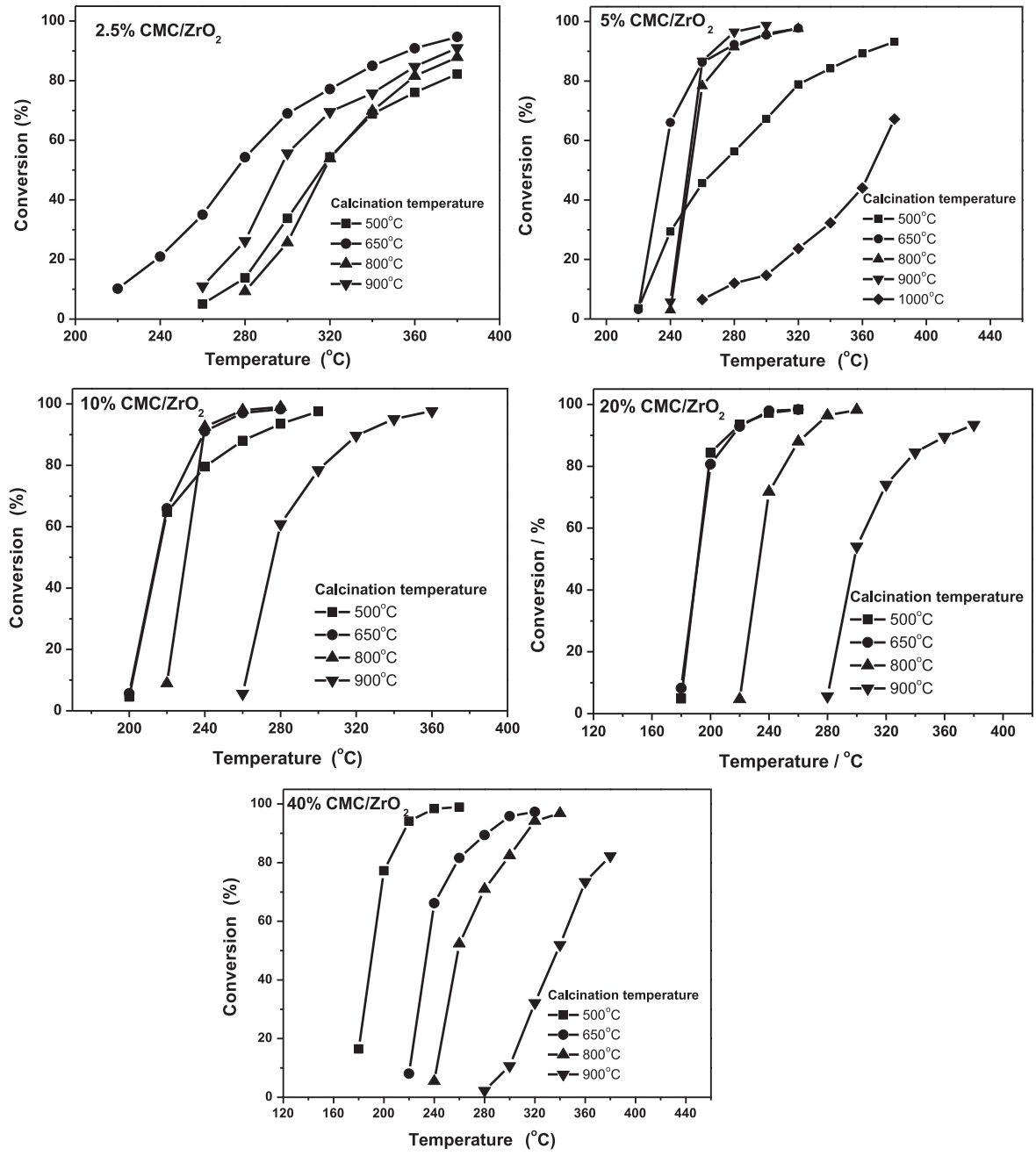

Fig. 1. The light-off curves of toluene combustion over CMC/ZrO_2 catalysts calcined at 500, 650, 800 900, and 1000 °C with CMC loading of 2.5%, 5.0%, 10.0%, 20.0% and 40.0%.

oxides catalysts [35,36], with similar surface area (72 m^2/g) to that of ZrO_2 (65 m^2/g), was used as the carrier for CMC catalyst. 5% and 20% CMC/TiO_2 catalysts were also prepared by the same method, and their activities were also evaluated in catalytic combustion of toluene (see Fig. 2). Similar to that of CMC/ZrO_2, the high activity is also observed in CMC/TiO_2 following calcination at 500 °C, which means that surface CMC dispersed on support are responsible for toluene combustion. Unlike ZrO_2, in Fig. 2, it is observed that the activity of CMC/TiO_2 drops sharply with the increase of calcination temperature. More interestingly, 5% CMC/TiO_2 seems more likely to sinter than 20% CMC/TiO_2, which is totally different from the case of CMC/ZrO_2. Therefore, based on the evidence of activity of CMC/TiO_2, we suggest that surface dispersion may not be the main reason leading to the high thermal stability of CMC/ZrO_2.

3.2. Catalyst characterization

3.2.1. XRD characterization

In order to achieve a deep insight into the structure evolution in thermal treatment, X-ray powder diffraction experiments of the catalysts were carried out. In the XRD patterns of all catalysts, the phases of CuO and MnOx were not to be found, indicating that manganese and copper species could enter into the fluorite lattice of CeO_2 to form the structure of CeO_2 solid solutions. However, the solubility limitation of Cu and Mn cations in CeO_2 reported by Aranda et al. [37] and Kang et al. [38] is to be less than 10 mol% highly depending on the preparation procedure. We suggest that the excessive amounts of Cu and Mn in CMC catalysts are dispersed on the surface of CeO_2 as CuO_x, MnO_x and their mixed oxides. Fig. 3 presents the XRD patterns of 5% and 40%

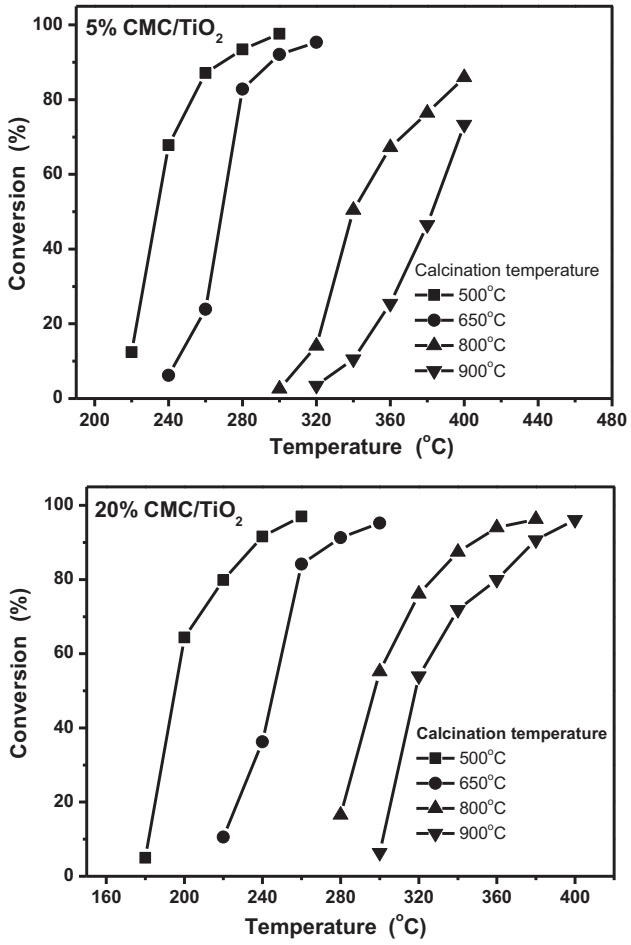

Fig. 2. The light-off curves of toluene combustion over CMC/TiO_2 catalysts calcined at 500, 650, 800 and 900 °C with CMC loading of 5.0% and 20.0%.

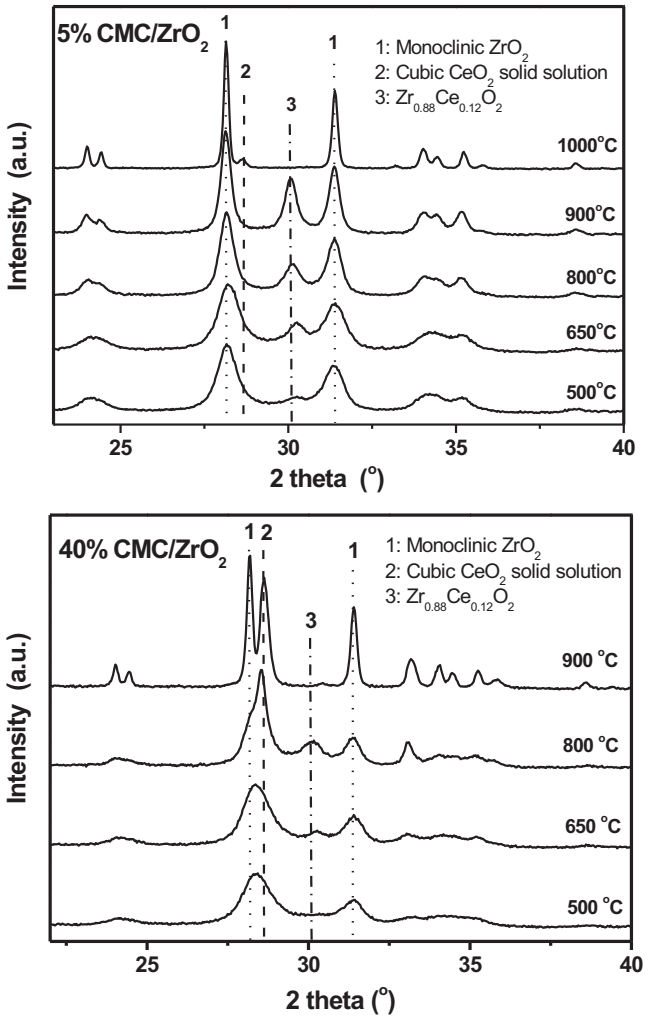

Fig. 3. XRD patterns of 5% and 40% CMC/ZrO_2 catalysts calcined at different temperatures.

CMC/ZrO_2 calcined at different temperatures. In the XRD patterns of 5% CMC/ZrO_2 calcined at 500–650 °C, only some major diffraction peaks at $2\theta = 28.34°$, 31.48° are detected, which are attributed to the monoclinic ZrO_2 structure (JCPDS 80-0966), indicating that CMC oxides is uniformly dispersed on ZrO_2. However, with further treated at 650 °C, a new weak peak at $2\theta = 30.0°$ is observed for 5% CMC/ZrO_2 which is attributed to the tetragonal $Zr_{0.88}Ce_{0.12}O_2$ solid solution structure (JSPDS 82-1398). The crystallization of $Zr_{0.88}Ce_{0.12}O_2$ is obviously improved following calcination at 900 °C under the interaction of ZrO_2 and CMC mixed oxides. However, with further increase in calcination temperature to 1000 °C, the diffraction peak of $Zr_{0.88}Ce_{0.12}O_2$ disappears, and another weak peak at $2\theta = 28.54°$ which is attributed to cubic CeO_2 fluorite structure (JCPDS 34-0394) evolves, that means dramatically sintering of the active CMC oxides particles on the surface of ZrO_2, and result in Ce^{4+} of $Zr_{0.88}Ce_{0.12}O_2$ return into CMC oxides structure.

The XRD patterns of 40% CMC/ZrO_2 catalyst calcined at 500–800 °C reveals a broad reflection at 2θ between 28.0° and 29.0° due to the overlapping diffraction of monoclinic ZrO_2 and cubic CeO_2. These two peaks are separated when the catalyst is further calcined at 900 °C due to increase of CMC oxides particles. The $Zr_{0.88}Ce_{0.12}O_2$ is observed from the samples which were calcined at 650 and 800 °C with much weaker intensity of diffraction than that of 5% CMC/ZrO_2. Following calcinations at 900 °C, $Zr_{0.88}Ce_{0.12}O_2$ disappears again. It is obvious that the higher loading will weaken the interaction between the solid phase of CMC and ZrO_2.

As a comparison, the XRD patterns of 20% CMC/TiO_2 samples calcined at 500 °C and 800 °C are shown in Fig. 4. It is found that only diffraction patterns corresponding to those of the cubic CeO_2 and TiO_2 are identified and no new mixed phases are observed. After calcination at 800 °C, the diffraction line intensity of cubic CeO_2 increases obviously and anatase TiO_2 undertakes

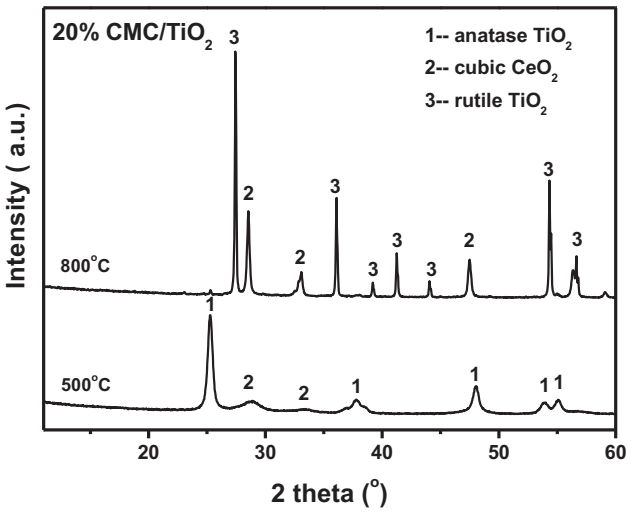

Fig. 4. XRD patterns of 20% CMC/TiO_2 catalysts calcined at 500 °C and 800 °C.

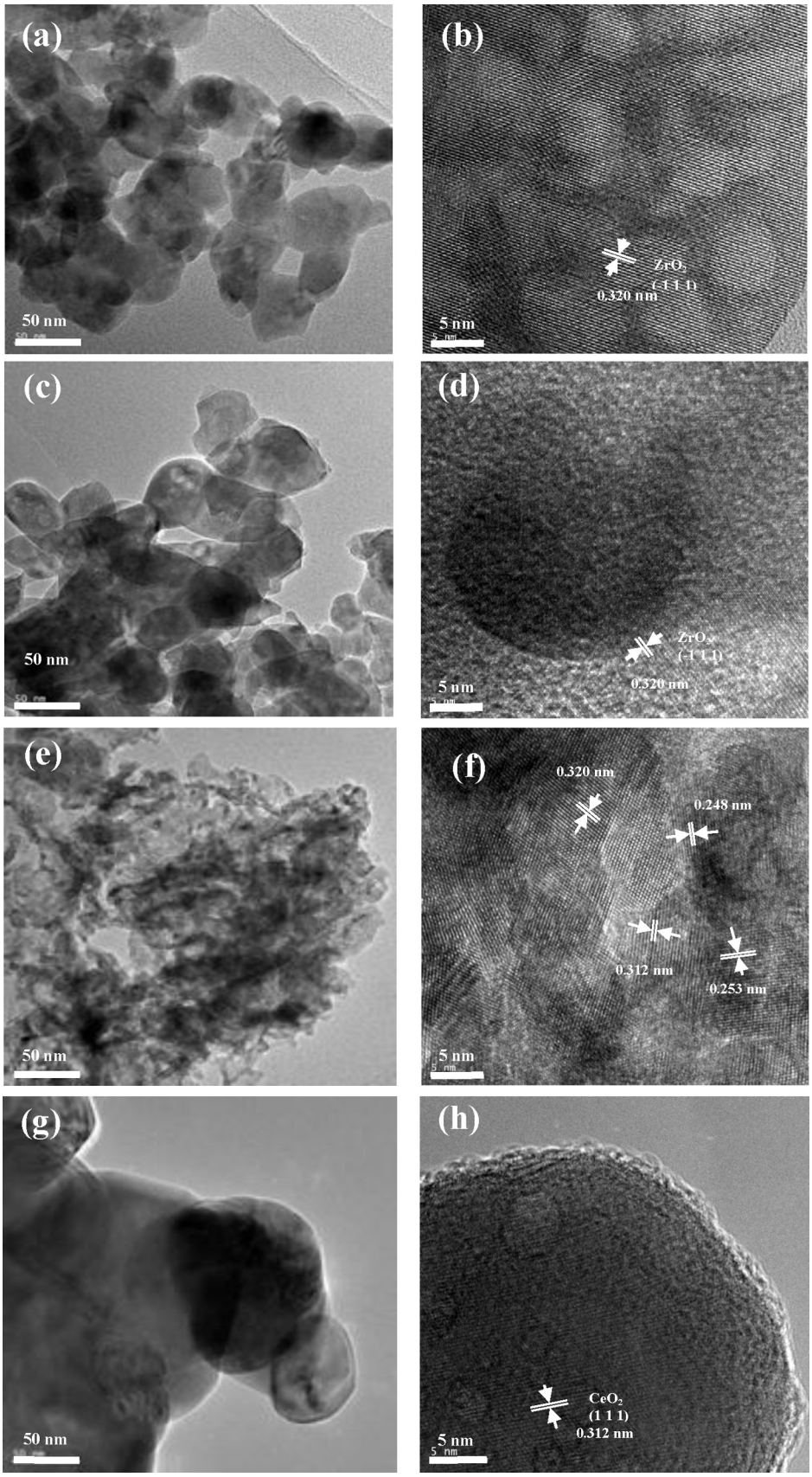

Fig. 5. TEM micrographs of CMC/ZrO_2. (a and b) 5% CMC/ZrO_2 calcined at 500 °C, (c and d) 5% CMC/ZrO_2 calcined at 900 °C, (e and f) 40% CMC/ZrO_2 calcined at 500 °C, (g and h) 40% CMC/ZrO_2 calcined at 900 °C.

phase transformation. Comparing these results with catalytic activity of CMC/ZrO_2, we suggest that severe sintering and deactivation of CMC/ZrO_2 is always accompanied by the disappearance of $Zr_{0.88}Ce_{.12}O_2$. Most probably, $Zr_{0.88}Ce_{.12}O_2$ existing in the interface plays a key role in stabilizing the active phase of CMC at high temperatures. However, excessive amounts of CMC over the surface of ZrO_2 do not necessarily lead to the formation of $Zr_{0.88}Ce_{.12}O_2$. Higher loading of CMC is more likely to sinter at relatively low temperatures and results in the separation of Ce^{4+} and Zr^{4+} in the interface and finally the disappearance of $Zr_{0.88}Ce_{12}O_2$.

3.2.2. HRTEM

The HRTEM images of 5% and 40% CMC/ZrO_2 calcined at 500 °C and 900 °C are illustrated in Fig. 5. The results confirm that these two catalysts are significantly different from each other in the size of particle and morphology. The particles of 5% CMC/ZrO_2 are uniform with the size distribution between 50 and 100 nm, and no noticeable changes in morphology are detected after calcination at 900 °C. Contrarily, in the HRTEM image of 5% CMC/ZrO_2-900 sample (see Fig. 5(d)), clearly, there is a mosaic of ceria-mixed oxides over the (−1 1 1) crystal plane of ZrO_2. The Ce^{4+} is inserted into the lattice of ZrO_2 under the thermal treatment, and leads to a change of crystal plane of ZrO_2, indicating the strong interaction of ZrO_2 and CeO_2.

The HRTEM characterization has also been conducted to detect the actual phase of 40% CMC/ZrO_2-500 catalysts in Fig. 5(f). The HRTEM image clearly shows several lattice fringes of the crystallinity of oxides, with an interplanar distance of 0.320 nm, indexed to the (−1 1 1) crystal plane of monoclinic ZrO_2, and the interplanar distance of 0.312 nm indexed to the (1 1 1) crystal plane of cubic CeO_2. In addition, some smaller lattice fringes are observed, with the lattice spaces of the (1 1 −1) crystal plane of monoclinic CuO and (2 1 1) crystal plane of tetragonal Mn_3O_4 estimated to be 0.253 nm and 0.248 nm respectively, which are rather close to that of the standard CuO sample (JCPDS 48-1548) and Mn_3O_4 sample (JCPDS 24-0734). These results confirm our previous assumption that the excessive amounts of Cu and Mn in CMC catalysts are dispersed on the surface of CeO_2 as CuO_x and MnO_x or their mixed oxides. However, after calcination at 900 °C, the size of 40% CMC/ZrO_2 particles increase dramatically, and the crystal planes of ZrO_2, CuO and Mn_3O_4 disappeared except CeO_2 oxides.

3.2.3. H_2-TPR experiments

The redox properties of 5% and 40% CMC/ZrO_2 were also investigated by H_2-TPR technique (see Fig. 6), and the relevant data are summarized in Table 1. Only one broad peak with peak temperature at about 200 °C is observed on CMC/ZrO_2 calcined at low temperatures. This reduction temperature (200 °C) is much lower than that of single Cu, Mn and Ce oxides [4,39], which further confirmed that there is a CeO_2 solid solution structure of Cu–Mn–Ce existing in the surface of ZrO_2. It has been widely reported that the reduction temperature of CeO_2 decreases obviously, when CeO_2 is doped with other metal ions [9,40,41]. Surprisingly, as shown in Fig. 6, the initial reduction temperature of 5% CMC/ZrO_2 gradually decreases with calcination temperature, implying the improvement of mobility of active oxygen species after calcination at high temperatures. This result is contrary to the common understanding that metal oxides are more difficult to be reduced after calcination at high temperatures due to the decrease in surface area [16,17,40]. According to XRD results, it is suggested that a decrease in reduction temperature is probably closely related to the formation of new $Zr_{0.88}Ce_{0.12}O_2$ phase. During thermal treatment, Ce^{4+} of CeO_2-based mixed oxide of CMC would enter into the lattice of ZrO_2, which may then result in the formation of some new lattice defects and an increase of oxygen vacancies in the active phase of CMC. In addition, the Cu–Mn mixed oxides which have been considered to

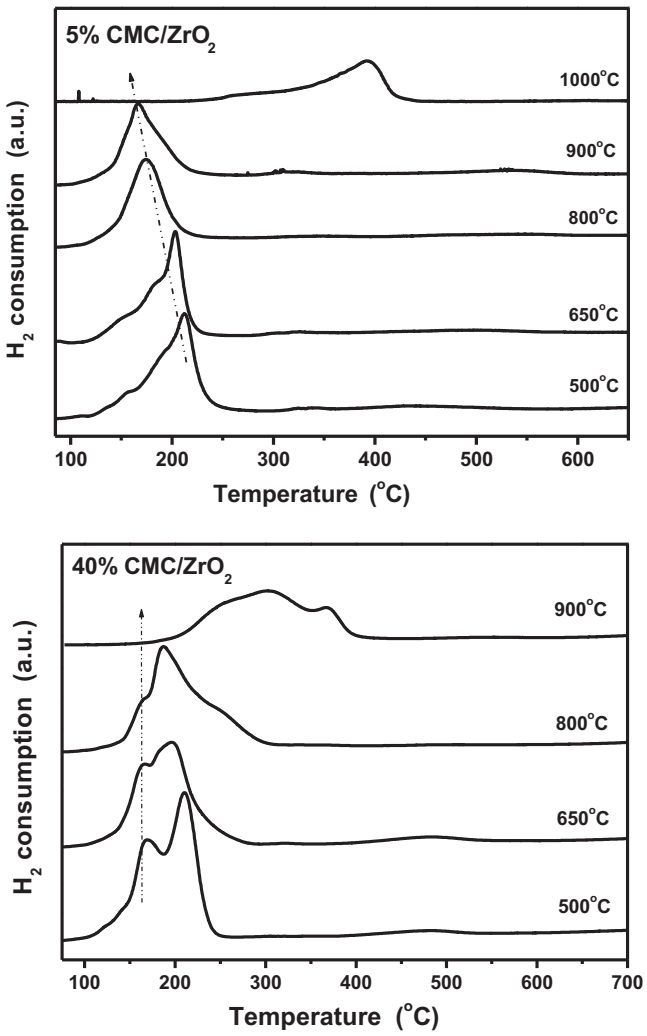

Fig. 6. H_2-TPR profiles of 5% and 40% CMC/ZrO_2 catalysts calcined at 500, 650, 800, 900 and 1000 °C.

be the active sites for oxidation reaction [39,42] would form more on the surface of the catalyst. On the contrary, the H_2-reduction process of 40% CMC/ZrO_2 is similar to the traditional metal oxide catalysts. Due to the sintering of surface CMC, the reduction peaks at temperature of around 160 °C become smaller with increase in calcination temperature. Therefore, it is reasonable to attribute the high activity of CMC catalyst to double active structures, namely, Cu and Mn oxides or their mixed oxides structure for activation of organic molecules during reaction, and ceria-based solid solution structure for the transportation of active oxygen including the surface and lattice oxygen.

To understand the effect of CMC loading on reducibility of catalysts, CMC/ZrO_2 catalysts loaded with different amounts of CMC were also investigated by H_2-TPR (see Fig. 7). Interestingly, the H_2-reduction peaks of catalysts calcined at 500 °C move to lower temperatures with increase of CMC loading. But for catalysts calcined at 900 °C, catalysts with lower loading of CMC have lower reduction temperatures. This result fully confirms that there is a strong solid-solid interaction between ZrO_2 and CeO_2, due to their similar ionic radius. Combining TPR profiles with the activities of catalysts, we propose that the H_2-consumption of reduction at the temperature range of 150–200 °C has direct relation with activity of the corresponding catalyst. Namely, the active surface oxygen which is reduced at low temperatures is the key factor responsible for activity in catalytic combustion. In addition, the reduction

Table 1
Surface area, hydrogen consumption (TPR) and reduction degree over CMC/ZrO_2 catalysts.

Samples	Calcination temperature[a] (°C)	BET m^2/g	Reduction temperature[b] (°C)	H_2 consumption[c] (mmol/g)	Reduction degree (χ) CMC-$O_{2-\chi}$
5% CMC/ZrO_2	500	52.3	215	0.217	0.647
	650	43.5	205	0.191	0.570
	800	21.8	175	0.171	0.510
	900	11.5	165	0.165	0.492
10% CMC/ZrO_2	500	47.5	175	0.400	0.624
	900	3.70	190	0.300	0.468
20% CMC/ZrO_2	500	48.6	165	0.684	0.583
	900	2.22	205	0.484	0.413
40% CMC/ZrO_2	500	47.2	165	1.027	0.510
	650	15.6	180	0.893	0.443
	800	6.54	190	0.833	0.414
	900	0.46	300	0.783	0.389

[a] All the catalysts were calcined at the corresponding temperatures for 3 h respectively.
[b] Temperature of the first reduction peak in TPR profile.
[c] CuO powder was used as the standard sample for the quantification of H_2 consumption during TPR experiments.

degrees (χ) of catalysts are also listed in Table 1. The catalysts with lower loadings have higher degrees of reduction, indicating that utilization of surface active oxygen would be enhanced by dispersion effect by ZrO_2 support.

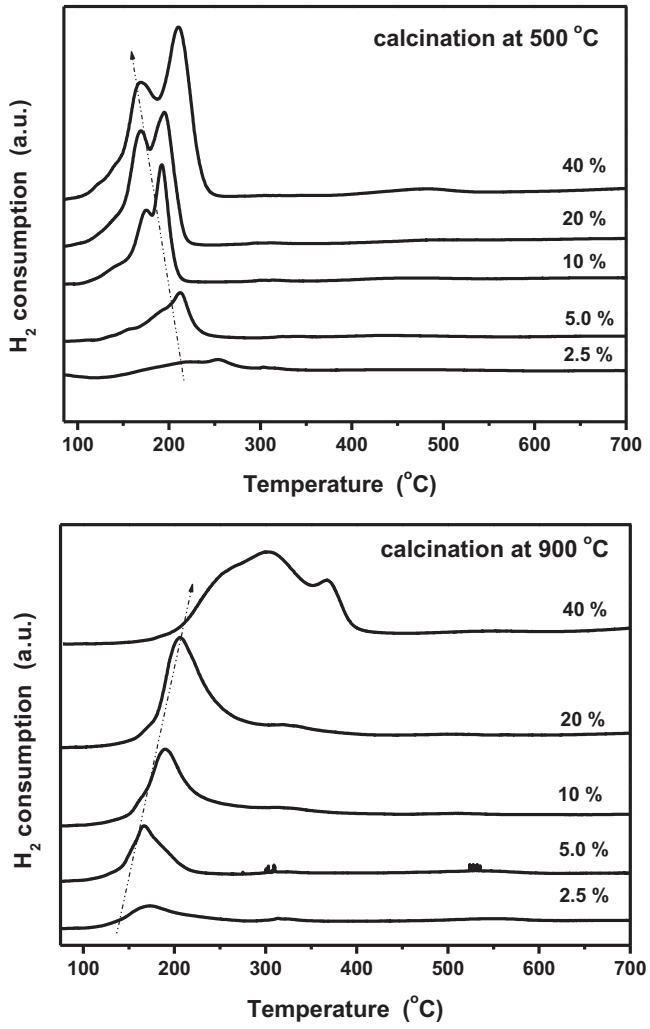

Fig. 7. H_2-TPR profiles of CMC/ZrO_2 catalysts with 2.5%, 5.0%, 10.0%, 20.0% and 40.0% CMC loading (all of them were calcined at 500 °C or 900 °C, respectively).

3.2.4. XPS characterization

The O_{1s} XPS spectra of 5% and 40% CMC/ZrO_2 calcined at 500 °C and 900 °C are presented in Fig. 8, and the relevant data are summarized in Table 2. The O_{1s} XPS spectra can be resolved into three peaks [3,16,40]: lattice oxygen (O_{latt}) at 529–530 eV, surface oxygen (O_{sur}) at 530–532 eV, which is assigned to defect oxide or the surface oxygen ions with low coordination situation and weakly bonded oxygen species, and adsorbed oxygen species (O_{ads}) at 533–534 eV from hydroxyl species and adsorbed water species as contaminants on the surface. For 5% CMC/ZrO_2 catalyst, following calcinations, the

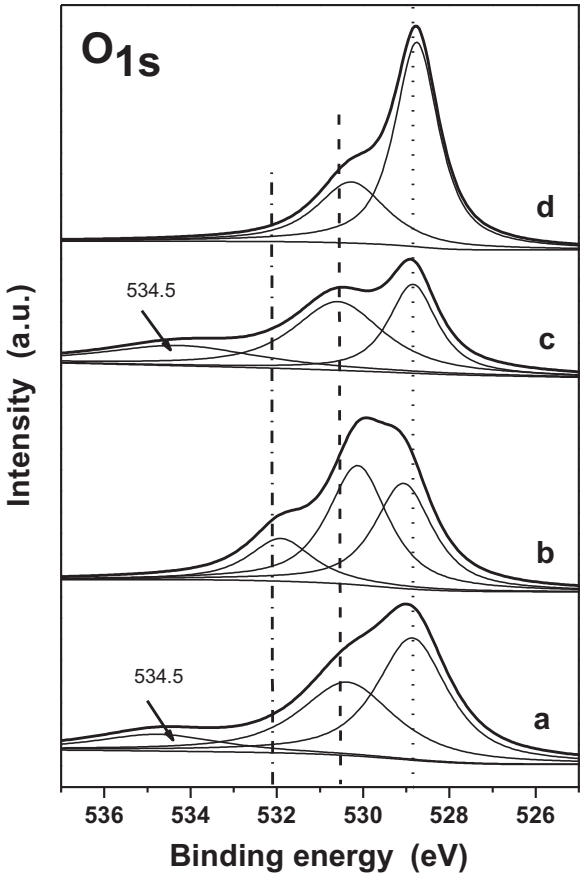

Fig. 8. O1s XPS spectra of the CMC/ZrO_2 catalysts. (a) 5% CMC/ZrO_2 calcined at 500 °C, (b) 5% CMC/ZrO_2 calcined at 900 °C, (c) 40% CMC/ZrO_2 calcined at 500 °C, and (d) 40% CMC/ZrO_2 calcined at 900 °C.

Table 2
The XPS results of 5% and 40% CMC/ZrO_2 calcined at 500 °C and 900 °C.

Catalysts	Calcination temperature	at %[a]			O_{1s} BE (eV)			
		Cu	Mn	Ce	O_{latt}	O_{sur}	O_{ads}	O_{sur}/O_{total}
5% CMC/ZrO_2	500	18.9	28.3	52.8	528.9	530.4	534.8	39.0
	900	29.4	35.2	35.4	529.1	530.1–531.9	/	61.7
40% CMC/ZrO_2	500	10.8	18.8	70.4	528.8	530.6	534.2	44.9
	900	15.1	22.7	62.2	529.4	530.9	/	31.9

[a] Obtained from the XPS analyses.

intensity and position of binding energy (BE) has not been changed significantly except for the disappearance of the O_{ads} peak. But the proportion of O_{sur} increases from 39.0% to 61.7% after calcination at 900 °C, which means that there is more active oxygen that could participate in oxidation reaction at low temperatures following Mar-van Krevelen mechanism. However, for 40% CMC/ZrO_2, the proportion of O_{sur} drops from 44.9% to 31.9% after calcination at 900 °C, and the intensity of O_{latt} obviously is enhanced due to the surface sintering of CMC mixed oxides.

The surface compositions of catalysts calcined at 500 °C and 900 °C might are compared and presented in Table 2. Ce content in the surface of 5% CMC/ZrO_2 is much lower that of 40% CMC/ZrO_2. This result can be explained by a strong interaction between ZrO_2 and CeO_2 in 5% CMC/ZrO_2, and Ce entering into the interface of catalyst. After calcination at 900 °C, the surface Ce content further decreases, confirming again that calcinations lead to the migration of Ce species toward the interface along with formation of a new phase of $Zr_{0.88}Ce_{0.12}O_2$. On the other hand, in 40% CMC/ZrO_2 catalysts, the surface Ce content keeps high value, close to the theoretical content. This result further reveals that high loading of CMC is not beneficial to the formation of an interface phase, and facilely sinters at high temperatures.

4. Conclusion

In summary, highly active CeO_2-based oxide as a substitute of expensive noble metal catalysts is attempted to be applied in more and more catalytic reactions, such as catalytic combustion, TWC and SCR. Unfortunately, its poor thermal stability limits its wide application in industry. Loading CeO_2-based mixed oxides on ZrO_2 is a simple and effective method to improve the thermal stability of catalyst. Especially for the exothermic oxidation reactions, ZrO_2 carrier cannot only stabilize the surface active structure of CeO_2-based oxides by formation of $Zr_{0.88}Ce_{0.12}O_2$ solid solution in the interface, but also can enhance mobility of active oxygen and improve catalytic performance of total oxidation. In addition, under conditions of oxidation reactions, the contradiction between activity and thermal stability of catalysts can be avoided by adjusting the loading of CeO_2-based mixed oxides, which provides a novel solution to prepare appropriate catalysts for specific oxidation reactions.

Acknowledgments

We would like to acknowledge the financial support from the Natural Science Foundation of China (No. 21107096) and the Commission of Science and Technology of Zhejiang province (No. 200713042).

References

[1] Q. Dai, H. Huang, Y. Zhu, W. Deng, S. Bai, X. Wang, G. Lu, Appl. Catal. B: Environ. 117 (2012) 360–368.
[2] H.F. Lu, Y. Zhou, H.F. Huang, B. Zhang, Y.F. Chen, J. Rare Earths 29 (2011) 855–860.
[3] H. Li, G. Lu, Q. Dai, Y. Wang, Y. Guo, Y. Guo, Appl. Catal. B: Environ. 102 (2011) 475–483.
[4] X.Y. Wang, Q. Kang, D. Li, Appl. Catal. B: Environ. 86 (2009) 166–175.
[5] D. Terribile, A. Trovarelli, C. de Leitenburg, A. Primavera, G. Dolcetti, Catal. Today 47 (1999) 133–140.
[6] X.Y. Wang, Q. Kang, D. Li, Catal. Commun. 9 (2008) 2158–2162.
[7] H.D. Liu, L.Q. Wei, R.L. Yue, Y.F. Chen, Catal. Commun. 11 (2010) 829–833.
[8] R.B. Jin, Y. Liu, Z.B. Wu, H.Q. Wang, T.T. Gu, Chemosphere 78 (2010) 1160–1166.
[9] P.A. Kumar, M.D. Tanwar, N. Russo, R. Pirone, D. Fino, Catal. Today 184 (2012) 279–287.
[10] X. Wu, F. Lin, L. Wang, D. Weng, Z. Zhou, J. Environ. Sci. 23 (2011) 1205–1210.
[11] M. Dhakad, T. Mitshuhashi, S. Rayalu, P. Doggali, S. Bakardjiva, J. Subrt, D. Fino, H. Haneda, N. Labhsetwar, Catal. Today 132 (2008) 188–193.
[12] M. Pijolat, M. Prin, M. Soustelle, O. Touret, P. Nortier, J. Chem. Soc., Faraday Trans. 91 (1995) 3941–3948.
[13] V. Perrichon, A. Laachir, S. Abouarnadasse, O. Touret, G. Blanchard, Appl. Catal. A: Gen. 129 (1995) 69–82.
[14] V.K. Ivanov, O.S. Polezhaeva, A.E. Baranchikov, A.B. Shcherbakov, Inorg. Mater. 46 (2010) 43–46.
[15] R. Si, Y.-W. Zhang, L.-M. Wang, S.-J. Li, B.-X. Lin, W.-S. Chu, Z.-Y. Wu, C.-H. Yan, J. Phys. Chem. C 111 (2007) 787–794.
[16] X.F. Tang, Y.G. Li, X.M. Huang, Y.D. Xu, H.Q. Zhu, J.G. Wang, W.J. Shen, Appl. Catal. B: Environ. 62 (2006) 265–273.
[17] X. Wu, S. Liu, D. Weng, F. Lin, R. Ran, J. Hazard Mater. 187 (2011) 283–290.
[18] F.Y. Wang, G.B. Jung, A. Su, S.H. Chan, X.A. Li, M. Duan, Y.C. Chiang, Mater. Lett. 63 (2009) 952–954.
[19] X. Wang, G. Lu, Y. Guo, L. Jiang, Y. Guo, C. Li, J. Mater. Sci. 44 (2009) 1294–1301.
[20] S. Sun, W. Chu, W. Yang, Chinese J. Catal. 30 (2009) 685–689.
[21] B. Zhao, G. Li, C. Ge, Q. Wang, R. Zhou, Appl. Catal. B: Environ. 96 (2010) 338–349.
[22] Q. Wang, B. Zhao, G. Li, R. Zhou, Environ. Sci. Technol. 44 (2010) 3870–3875.
[23] S. Damyanova, B. Pawelec, K. Arishtirova, M.V.M. Huerta, J.L.G. Fierro, Appl. Catal. A: Gen. 337 (2008) 86–96.
[24] M. Ozawa, M. Hattori, T. Yamaguchi, J. Alloys Compd. 451 (2008) 621–623.
[25] D.Q. Li, C. Gao, Y.J. Lin, Y. Li, D.G. Evans, Ind. Eng. Chem. Res. 48 (2009) 6544–6549.
[26] F. Huang, Y. Zheng, Z. Li, Y. Xiao, Y. Zheng, G. Cai, K. Wei, Chem. Commun. 47 (2011) 5247–5249.
[27] F.Z. Zhao, S.F. Ji, P.Y. Wu, Z.F. Li, C.Y. Li, Catal. Today 147 (2009) S215–S219.
[28] B.M. Reddy, P. Lakshmanan, A. Khan, S. Loridant, C. Lopez-Cartes, T.C. Rojas, A. Fernandez, J. Phys. Chem. B 109 (2005) 13545–13552.
[29] M.F. Luo, M. He, Y.L. Xie, P. Fang, L.Y. Jin, Appl. Catal. B: Environ. 69 (2007) 213–218.
[30] S.M. Saqer, D.I. Kondarides, X.E. Verykios, Top. Catal. 52 (2009) 517–527.
[31] J.G. Deng, H.X. Dai, H.Y. Jiang, L. Zhang, G.Z. Wang, H. He, C.T. Au, Environ. Sci. Technol. 44 (2010) 2618–2623.
[32] J.G. Deng, L. Zhang, H.X. Dai, H. He, C.T. Au, Ind. Eng. Chem. Res. 47 (2008) 8175–8183.
[33] Y.G. Wang, J.W. Ren, Y.Q. Wang, F.Y. Zhang, X.H. Liu, Y. Guo, G.Z. Lu, J. Phys. Chem. C 112 (2008) 15293–15298.
[34] H. Shimokawa, H. Kusaba, H. Einaga, Y. Teraoka, Catal. Today 139 (2008) 8–14.
[35] D.Q. Yu, Y. Liu, Z.B.A. Wu, Catal. Commun. 11 (2010) 788–791.
[36] V.H. Vu, J. Belkouch, A. Ould-Dris, B. Taouk, AIChE J. 54 (2008) 1585–1591.
[37] A. Aranda, E. Aylo, B. Solsona, R. Murillo, A. Mastral, D. Sellick, A. Said, T. Garcı, S. Taylor, Chem Commun. 48 (2012) 4704–4706.
[38] C.Y. Kang, H. Kusaba, H. Yahiro, K. Sasaki, Y. Teraoka, Solid State Ionics 177 (2006) 1799–1802.
[39] M.R. Morales, B.P. Barbero, L.E. Cadus, Fuel 87 (2008) 1177–1186.
[40] X.F. Tang, Y.D. Xu, W.J. Shen, Chem. Eng. J. 144 (2008) 175–180.
[41] M. O'Connell, M.A. Morris, Catal. Today 59 (2000) 387–393.
[42] M.R. Morales, B.P. Barbero, L.E. Cadus, Appl. Catal. B: Environ. 67 (2006) 229–236.